LETTERS

Arctic freshwater forcing of the Younger Dryas cold reversal

Lev Tarasov[1] & W.R. Peltier[1]

The last deglaciation was abruptly interrupted by a millennial-scale reversal to glacial conditions[1], the Younger Dryas cold event. This cold interval has been connected to a decrease in the rate of North Atlantic Deep Water formation and to a resulting weakening of the meridional overturning circulation[2–4] owing to surface water freshening. In contrast, an earlier input of fresh water (meltwater pulse 1a), whose origin is disputed[5,6], apparently did not lead to a reduction of the meridional overturning circulation[4]. Here we analyse an ensemble of simulations of the drainage chronology of the North American ice sheet in order to identify the geographical release points of freshwater forcing during deglaciation. According to the simulations with our calibrated glacial systems model, the North American ice sheet contributed about half the fresh water of meltwater pulse 1a. During the onset of the Younger Dryas, we find that the largest combined meltwater/iceberg discharge was directed into the Arctic Ocean. Given that the only drainage outlet from the Arctic Ocean was via the Fram Strait into the Greenland–Iceland–Norwegian seas[7], where North Atlantic Deep Water is formed today, we hypothesize that it was this Arctic freshwater flux that triggered the Younger Dryas cold reversal.

Among the various mechanisms of climate change, those that are the most difficult to constrain and that may be the most severe are those associated with fast nonlinear processes. Abrupt and sustained changes in the thermohaline circulation (THC) have been implicated in past events of this kind, such as the Dansgaard–Oeschger oscillations that were a recurrent characteristic of marine isotope stage 3[1]. It has also been suggested that similarly rapid changes in the meridional overturning circulation (MOC) could occur in response to global warming[8]. However, the actual sensitivity of North Atlantic Deep Water formation and MOC to freshwater forcing remains poorly understood. As the most recent strong millennial-scale response to a variation in the MOC, the Younger Dryas (YD) event offers a basis for a clear test of the sensitivity of North Atlantic Deep Water formation to freshwater fluxes. In order to perform this test, however, a detailed deglacial chronology of the runoff of fresh water from the continents is required. Here we analyse the largest possible contribution, that from the disintegration of the North American ice sheet (NAIS) complex.

A significant challenge to the hypothesis that it was extreme meltwater forcing that triggered the YD concerns our understanding of meltwater pulse 1a (mwp-1a). This event produced a rise of approximately 20 m in eustatic sea level over an interval of 500 yr (see below), during which no significant decrease in the MOC has been inferred[4]. $\delta^{18}O$ records from the Gulf of Mexico indicate that a large contribution to mwp-1a entered the Gulf (via the Mississippi River outlet, Fig. 1), and it has been suggested on the basis of models that such a freshwater flux would thereafter be advected into the North Atlantic by the Gulf Stream, with a resultant significant diminishing of the MOC[9]. The eustatic sea level record during the onset of the YD, on the other hand, lacks a discernible meltwater pulse (Fig. 2). Reconstructed sea surface salinities for the Gulf of St Lawrence[10] have also refuted the presence of a surface meltwater plume in this region during the period of YD onset, contradicting a previous hypothesis[11]. Two fundamental fluid dynamical issues (see Supplementary Information) concerning the hyperpycnal behaviour of sediment-laden riverine outflow into the oceans[12] and the strong baroclinic instability of the Gulf Stream also make it unlikely that discharge of melt water into the Atlantic Ocean or the Gulf of Mexico could produce a low-salinity surface plume that was advected intact to the sites of North Atlantic Deep Water formation.

In order to significantly influence the MOC, freshwater forcing must be applied directly onto the region of North Atlantic Deep Water formation—as apparently occurred during the Heinrich events, when the surface freshening was associated with the melting of icebergs expelled into the Atlantic from the NAIS by calving through the Hudson Strait[13]. One might expect to achieve the same effect by means of freshwater delivery, especially in the form of pack ice, through the Fram Strait into the Greenland–Iceland–Norwegian (GIN) seas (Fig. 1), as has been previously hypothesized for the Preboreal Oscillation[14]. Indeed, four planktonic $\delta^{18}O$ data points from three sedimentary cores (PS2837, PS2887, PS1230) in the western Fram Strait[15,16] collectively appear to indicate the presence of such an event between 10.5 and 11.2 ^{14}C kyr ago (bracketing YD onset). Our analyses demonstrate this alternative mechanism to be the preferred candidate for the cause of the YD.

In order to reconstruct a regional deglacial drainage chronology for North America that (to our knowledge, for the first time) includes an objective (though incomplete) measure of uncertainty, we use a best-fit 77 member sub-ensemble from a 5,000 member ensemble of glacial systems model (GSM) analyses[17], calibrated against an extensive set of relative-sea-level and geodetic observations using a bayesian methodology. To further reduce uncertainties, the model is forced to conform to a newly developed high-resolution margin chronology derived from ^{14}C dated geological and geomorphological observations[7,18].

In comparing the computed deglacial contribution of the NAIS to the palaeorecord of eustatic sea level change (Fig. 2), four key points emerge. First, the GSM explains approximately half of the 20 m eustatic sea level rise associated with the mwp-1a event. Second, there is no similarly intense meltwater pulse predicted during the onset of the YD. Third, the model produces no significant contribution to mwp-1b. Fourth, as is demonstrated below, although discharge into the Gulf of Mexico and the Atlantic Ocean are the dominant contributions of the NAIS to mwp-1a, there is also substantial discharge into the Arctic Ocean (and the Pacific Ocean, though not shown here). Given the inferred collapse of the Barents Sea ice sheet during this interval[19] and the stronger response of the Eurasian ice sheet to climate forcing[20], it follows that a substantial fraction of the remaining contribution to mwp-1a is due to Eurasian sources.

[1]Department of Physics, University of Toronto, Toronto, Ontario, Canada M5S 1A7.

The lack of a direct connection between the eustatic sea level record and climate response during the period of YD onset implies that the most important factor in determining the effect of the freshwater forcing upon the MOC is not the total amount of melt water that enters the ocean basins but rather its regional distribution. Considering first the discharge into the Gulf of Mexico (Fig. 3a), the largest deglacial meltwater pulse (1.35 ± 0.4 dSv 100 yr mean, 1.65 ± 0.25 dSv after eliminating simulations with apparently unsupported Eastern routeing of Lake Agassiz drainage; 1 dSv = 10^5 m^3 s^{-1}) is predicted to have occurred during the mwp-1a event, as previously inferred on the basis of the Orca basin $\delta^{18}O$ record[11]. Southern meltwater discharge terminates by −12.9 kyr (that is, 12.9 kyr before present).

The largest total discharge into the Atlantic Ocean through a mid-latitude outlet (that is, not including the Labrador Sea) also occurs during the mwp-1a interval with a 1σ range of 1.0–1.9 dSv (Fig. 3b). Discharge into the mid-Atlantic is split between the Hudson River outlet (0.5–1.4 dSv) and the Gulf of St Lawrence (0.5 dSv). During the YD interval, significant discharge occurs only via the Gulf of St Lawrence, and has a 1σ range of 0.1–0.4 dSv (meltwater and iceberg flux only, up to 0.7 dSv including precipitation over ice-free land). Mean North American discharge into the Labrador Sea during the YD interval is, except for a peak of 0.2 dSv at −12.8 kyr, below 0.1 dSv until an imposed ice reduction representing an assumed Heinrich event H0 subsequent to −12.0 kyr.

Peak (100 yr weighted mean) ensemble discharge into the Arctic Ocean is 0.7 dSv during the mwp-1a interval (Fig. 3c). Most importantly, mean discharge first surpasses 1 dSv near −12.9 kyr and peaks at −12.8 kyr with a 1σ range of 1.2–2.2 dSv. This peak discharge into the Arctic Ocean is more than twice the sum total of all Atlantic discharge from the NAIS (including the Gulf of Mexico and the Labrador Sea) during the YD onset period. To place this in perspective, the present day outflow of the Mackenzie River is approximately 0.11 dSv, while the total present-day Arctic Ocean freshwater outflow through the Fram Strait is approximately 1.1 dSv (ref. 21). Given that our analyses ignore both Eurasian inputs into the Arctic Ocean (at present 1.0 dSv; ref. 21) and net precipitation over the Arctic Ocean (at present 0.3 dSv; ref. 21), the 1–2 dSv increase of North American freshwater flux into the Arctic during YD onset is highly significant. Furthermore, the actual discharge would have had significant higher frequency variability (and therefore higher peak values) than is evident with the 100 yr timesteps of the drainage calculations.

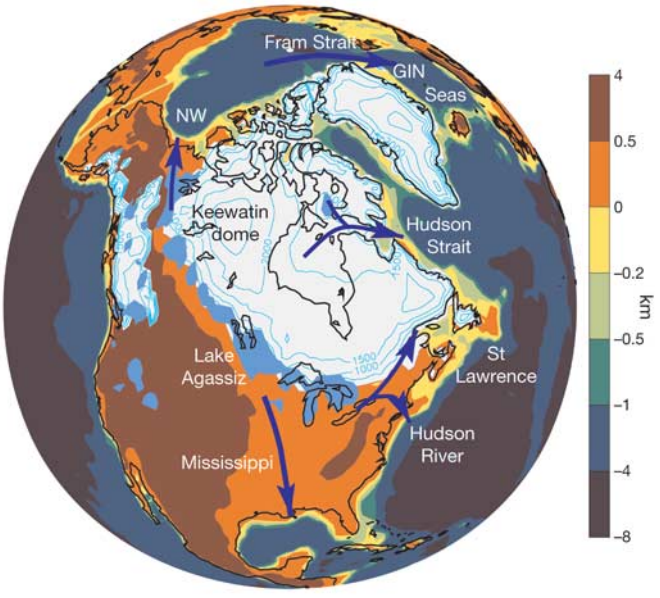

Figure 1 | Major deglacial drainage outlets for North America, along with approximate positions of proglacial Lake Agassiz and Keewatin dome just before the onset of the YD. Modern North Atlantic Deep Water formation primarily occurs in the GIN seas region. Northwest (NW) drainage of the ice complex is via the Mackenzie River basin into the Beaufort Sea and subsequently into the Canadian basin of the Arctic Ocean. Surface elevation is indicated by the colour scale.

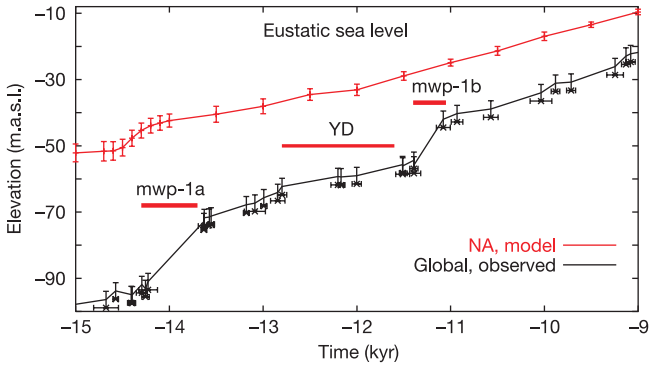

Figure 2 | Eustatic sea-level chronologies. Black curve, the observed chronology as inferred from the U/Th-dated Barbados *Acropora palmata* coral record[29]. Red curve, the computed North American contribution ('NA, model') to eustatic sea level rise as delivered by a 78 member best-fit sub-ensemble with 1σ confidence intervals as determined by fit to the data set employed to constrain the model. Not included are uncertainties associated with the margin chronology and the limited ensemble phase space. m.a.s.l., metres above sea level. The time intervals for the mwp-1a, YD, and mwp-1b events are delineated by the horizontal red bars.

Previous analyses using largely unconstrained deglacial chronologies lacking a Keewatin ice dome[22,23] have inferred substantial discharge into the Arctic Ocean only after termination of the YD. The timing of this intense period of freshwater forcing in our reconstruction is relatively insensitive to the uncertainty in deglacial climate chronology, in that use of the GISP II $\delta^{18}O$ record for the climate forcing chronology (Fig. 3d) does not modify the timing. Rather, the timing of this event is fixed by the margin chronology and therefore subject primarily to its uncertainties (as detailed in Supplementary Discussion). The continuous high-level discharge over the whole YD interval with the inclusion of precipitation over ice-free land ('Upper bound' in Fig. 3b) may also have played a critical role in sustaining MOC reduction for a millennium.

The underlying source of this strong discharge into the Arctic Ocean is the large Keewatin ice dome (Fig. 1), whose existence at the Last Glacial Maximum was recently confirmed through analyses of space geodetic and absolute gravity constraints[24,17]. The strength of local sourcing is evident in that even with the removal of all runs that have northwest drainage of Lake Agassiz at −12.8 kyr, ensemble discharge into the Arctic Ocean still dominates, with a 1σ range of 1.1–1.5 dSv. Our ensemble-based analyses do however indicate northwest drainage of Lake Agassiz during much or all of the YD, contrary to the eastward drainage that has until recently generally been assumed[25] but is now in question[26]. The −12.8 kyr Arctic meltwater (and iceberg) flux has contributions from both the reduction of the volume of this ice dome as well as from the expansion of the drainage basin due to the isostatic depression induced by this surface load. The magnitude of this primary dome of the Last Glacial Maximum NAIS is determined by two significant constraints in the calibrated model. The recently refined observation of the rate (6.5 ± 1.5 mm yr^{-1}) of present day uplift of the surface of the solid Earth based on very-long-baseline interferometry and GPS (Global Positioning System) measurements at Yellowknife (D. F. Argus, personal communication) provides a strong regional constraint. Furthermore, global ice volume constraints together with regional limits on the amount of ice that could have existed on other

continents (based on relative sea level and glaciological analyses along with inferred ice margin chronologies) require a substantial ice load over North America, which on the basis of relative sea level observations implies large ice volume over the Keewatin region. It is also noteworthy that a large Keewatin dome was previously inferred on the basis of glacial geomorphology[27].

Detailed understanding of the physical process by which the freshwater flux into the Arctic Ocean affects the Atlantic MOC will require further investigation. Given the strong stable stratification that is characteristic of Arctic waters[21], it may be that a significant surface meltwater plume was simply advected through the Fram Strait directly into the GIN seas. However, the enhanced freshwater flux would also have increased sea ice formation in the Arctic, with a resultant enhanced flux of pack ice into the GIN seas. Given that ice transport through the Fram Strait at present accounts for three-quarters of the mean annual freshwater export from the Arctic Ocean through the Fram Strait (0.9 dSv; ref. 21), with mean monthly discharge in the winter months (probably a better analogue for YD era annual conditions) at times greater than 2.4 dSv (ref. 28), we believe that this second mechanism of freshwater transport in combination with some iceberg flux played a dominant role during YD onset. Further testing of this 'Arctic trigger' hypothesis will require improved observational constraints on the deglacial chronology of the Keewatin ice dome, and detailed data from marine sedimentary cores from the Arctic basin (especially the Beaufort Sea region), along with numerical experiments to examine directly the response of coupled atmosphere–ocean general circulation models to the deglacial drainage chronology.

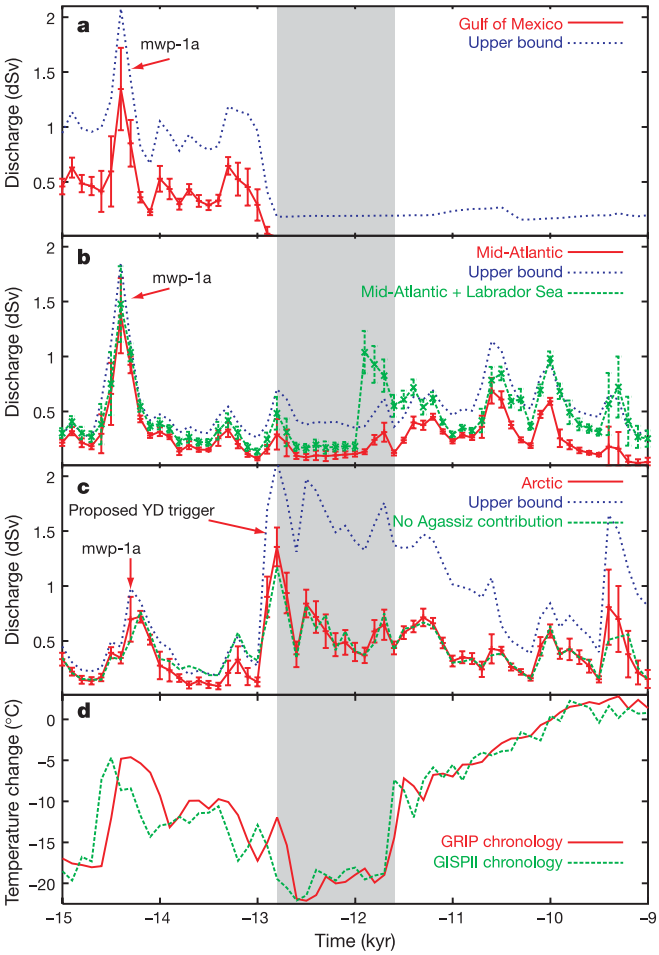

Figure 3 | Computed regional drainage chronologies and the inferred regional temperature change chronology. a–c, Computed regional drainage chronologies for the Gulf of Mexico (**a**), the Atlantic (**b**) and the Arctic (**c**). **d**, The inferred regional temperature change chronology from Central Greenland, from a calibrated glaciological model[30]. 'Mid-Atlantic' (**b**) is all discharge from Newfoundland to Georgia. 'No Agassiz contribution' (**c**) is the mean Arctic discharge for ensemble runs that have eastern drainage of Lake Agassiz at −12.8 kyr. The large scatter in Gulf of Mexico (**a**) and Atlantic (**b**) discharge at −14.4 kyr is due to variations in the routeing of Lake Agassiz drainage between eastern and southern outlets. The grey bar denotes the YD interval. Surface drainage is computed every 100 yr using mean meltwater (from the ice-sheet only) and iceberg fluxes over the 100 yr interval and the instantaneous surface topography. The 1σ confidence intervals shown are as per Fig. 2. 'Upper bound' denotes the 1σ upper bound with the additional inclusion of precipitation over ice-free land in the discharge calculation. Interpretation of these latter results requires recognition of the large uncertainties in estimated deglacial precipitation over ice-free land.

METHODS

GSM. The University of Toronto Glacial Systems Model (GSM) used for the analyses presented here incorporates a three-dimensional thermo-mechanically coupled ice-sheet model, bed-thermal model, sub-glacial till-deformation model, temperature-dependent positive degree-day mass-balance model with a physical refreezing parameterization, spherically symmetric visco-elastic isostatic response model, and a fast surface drainage solver. For the results presented here, the GSM was run at 1.0° longitude by 0.5° latitude grid resolution. A complete description of the GSM is provided elsewhere (ref. 17 and references therein), and only a brief summary is provided here.

The ice-sheet component of the GSM is based upon the standard Glen flow ice rheology and shallow ice approximation. Coulomb-plastic till deformation is assumed to occur when the basal temperature approaches the pressure-melting point and adequate sediment is available. The isostatic response model employs the VM2 radial mantle viscosity structure, the PREM radial elasticity model, and a 100-km-thick surface lithosphere (with infinite viscosity). A gravitationally self-consistent relative sea level solver[6] is applied in post-processing to compare model predictions to observations. The climate forcing used to drive the GSM is derived from the GRIP $\delta^{18}O$ record in combination with reconstructed isotopic sensitivity parameters to define a glacial index that is used to linearly interpolate between a glacial climate state derived from an ensemble of PMIP (Paleo Model Intercomparison Project, http://www-lsce.cea.fr/pmip/) general circulation model reconstructions of Last Glacial Maximum climate and a present day reanalysis-based climatology.

Model calibration. 22 ensemble parameters representing uncertainties in climate forcing, ice calving, and fast flow physics (including forced ice reduction during Heinrich events 1 and 0) are varied in a bayesian calibration (R. Neal, W.R.P and L.T., manuscript in preparation) of the GSM against a large set (over 5,540 data points) of relative-sea-level and geodetic observations. The bayesian calibration employs a multilayer perceptron neural network simulator of the GSM to extensively probe the model phase space. The posterior distribution for a parameter set given the constraint data set is proportional to the product of the prior probability distribution of the parameters and the probability of the observational constraint data given the parameters. Trial parameter sets are extracted by means of Markov Chain Monte Carlo (MCMC) sampling from this posterior distribution. These parameter sets are then applied to the full GSM. Subsequent results are employed to further train the neural network (using bayesian methods) for further iterative calibration. Each ensemble run covers a whole glacial cycle starting at −122 kyr (that is, the Eemian interglacial). The limited phase space of the GSM in combination with uncertainties in the applied margin chronology[7,18] and the regionally (and temporally) limited coverage of the constraint data set constitute the largest uncertainties that cannot be accounted for in the calibration procedure.

Surface drainage. The surface drainage solver diagnostically computes downslope drainage along with surface water storage using a two-stage depression-fill algorithm, and is run at the same spatial resolution as the rest of the GSM. In essence, the algorithm is quite simple: diagnostically let meltwater (averaged over 100 yr) flow down the contemporaneous surface slope at the end of the 100 yr diagnostic time-step, filling depressions (subject to available melt water), until it either enters a depression for which not enough melt water is available to overflow the depression, or until melt water reaches the deep ocean (defined as regions with present-day bathymetry deeper than 600 m). The meltwater discharge into each ocean basin (Pacific, Arctic, Labrador Sea, St Lawrence (Atlantic, south of Newfoundland and excluding Hudson River basin), Hudson River basin, Caribbean (Mississippi)) then follows from the summation of the meltwater fluxes into the deep-water sector of each basin. To provide a sense of

the range of drainage basin configurations for a single timeslice, computed −12.8 kyr drainage basins for three good-fit runs are shown in the Supplementary Figures. The algorithm assumes zero water depth across controlling sills. Meltwater and iceberg discharge are lumped together in the surface drainage determination. The drainage topography used in the GSM is derived from the high resolution hydrologically correct HYDRO1K digital elevation map (http://edcdaac.usgs.gov/gtopo30/hydro/namerica.asp) with local modifications based on sub-grid manual checks of critical drainage choke-points. A few critical choke-point elevations are taken to be time-dependent, to account for either sub-grid movement of the ice margin across the grid-cell (determined using linear interpolation between ice margin chronology time-slices across a much higher resolution version of the drainage topography) or erosional changes inferred on the basis of regional strandline data. Changes in surface water loading (excluding geoidal perturbations in the coupled model) are also accounted for in computing the isostatic adjustment of the solid Earth. The combined solver and drainage topography have been verified against a coarse-grained version of the level 1 drainage basins of the HYDRO1k data set.

Received 5 October 2004; accepted 1 April 2005.

1. Dansgaard, W. *et al.* Evidence for general instability of past climate from a 250 kyr ice-core record. *Nature* **264,** 218–220 (1993).
2. Keigwin, L. D., Jones, J. A., Lehman, S. J. & Boyle, E. A. Deglacial meltwater discharge, North-Atlantic deep circulation, and abrupt climate change. *J. Geophys. Res.* **96,** 16811–16826 (1991).
3. Muscheler, R., Beer, J., Wagner, G. & Finkel, R. Changes in deep-water formation during the Younger Dryas event inferred from ^{10}Be and ^{14}C records. *Nature* **408,** 567–570 (2000).
4. McManus, J. F., Francois, R., Gherardi, J.-M., Keigwin, L. D. & Brown-Leger, S. Collapse and rapid resumption of Atlantic meridional circulation linked to deglacial climate changes. *Nature* **428,** 834–837 (2004).
5. Clark, P. *et al.* Origin of the first global meltwater pulse following the last glacial maximum. *Paleoceanography* **11,** 563–577 (1996).
6. Peltier, W. R. On the hemispheric origins of meltwater pulse 1-a. *Quat. Sci. Rev.* (in the press).
7. Dyke, A. S. in *Quaternary Glaciations—Extent and Chronology*, Part II, Vol. 2b (eds Ehlers, J. & Gibbard, P. L.) 373–424 (Elsevier Science and Technology Books, Amsterdam, 2004).
8. Stocker, T. F. & Schmittner, A. Influence of carbon dioxide emission rates on the stability of the thermohaline circulation. *Nature* **388,** 862–865 (1997).
9. Manabe, S. & Stouffer, R. J. Coupled ocean-atmosphere model response to freshwater input: comparison to Younger Dryas event. *Paleoceanography* **12,** 321–336 (1997).
10. de Vernal, A., Hillaire-Marcel, C. & Bilodeau, G. Reduced meltwater outflow from the Laurentide ice margin during the Younger Dryas. *Nature* **381,** 774–777 (1996).
11. Broecker, W. S. *et al.* Routing of meltwater from the Laurentide Ice Sheet during the Younger Dryas cold episode. *Nature* **341,** 318–321 (1989).
12. Parsons, J. D., Bush, J. W. & Syvitski, J. P. Hyperpycnal plume formation from riverine outflows with small sediment concentrations. *Sedimentology* **48,** 465–478 (2001).
13. Hemming, S. R. Massive late Pleistocene detritus layers of the North Atlantic and their global climate imprint. *Rev. Geophys.* **42,** doi:10.1029/2003RG000128 (2004).
14. Fisher, T. G., Smith, D. G. & Andrews, J. T. Preboreal oscillation caused by a glacial Lake Agassiz flood. *Quat. Sci. Rev* **21,** 873–878 (2002).
15. Bauch, H. A. *et al.* A multiproxy reconstruction of the evolution of deep and surface waters in the subarctic Nordic seas over the last 30,000 yr. *Quat. Sci. Rev.* **20,** 659–678 (2001).
16. Norgaard-Pedersen, N. *et al.* Arctic Ocean during the Last Glacial Maximum: Atlantic and polar domains of surface water mass distribution and ice cover. *Paleoc.* **18,** doi:10.1029/2002PA000781 (2003).
17. Tarasov, L. & Peltier, W. R. A geophysically constrained large ensemble analysis of the deglacial history of the North American ice sheet complex. *Quat. Sci. Rev* **23,** 359–388 (2004).
18. Dyke, A. S., Moore, A. & Robertson, L. *Deglaciation of North America* (Tech. Rep. Open File 1574, Geological Survey of Canada, Ottawa, 2003).
19. Svendsen, J. I. *et al.* Late Quaternary ice sheet history of northern Eurasia. *Quat. Sci. Rev.* **23,** 1229–1271 (2004).
20. Tarasov, L. & Peltier, W. R. Terminating the 100 kyr ice age cycle. *J. Geophys. Res.* **102,** 21665–21693 (1997).
21. Aagaard, K. & Carmack, E. C. The role of sea ice and other fresh water in the Arctic circulation. *J. Geophys. Res.* **94,** 14485–14498 (1989).
22. Licciardi, J. M., Teller, J. T. & Clark, P. U. in *Mechanisms of Global Climate Change at Millennial Time Scales* (eds Clark, P. U., Webb, R. S. & Keigwin, L. D.) 177–201 (AGU Geophysical Monographs Vol. 112, American Geophysical Union, Washington DC, 1999).
23. Marshall, S. J. & Clarke, G. K. C. Modeling North American freshwater runoff through the last glacial cycle. *Quat. Res* **52,** 300–315 (1999).
24. Peltier, W. R. Global glacial isostatic adjustment: Paleo-geodetic and space-geodetic tests of the ICE-4G (VM2) model. *J. Quat. Sci.* **17,** 491–510 (2002).
25. Teller, J. T. & Leverington, D. W. Glacial Lake Agassiz: a 5000 yr history of change and its relationship to the δ^{18}O record of Greenland. *Geol. Soc. Am. Bull.* **116,** 729–742 (2004).
26. Teller, J. T., Boyd, M., Yang, Z., Kor, P. S. G. & Fard, A. M. Alternative routing of Lake Agassiz overflow during the Younger Dryas: New dates, paleotopography, and a reevaluation. *Quat. Sci. Rev.* (in the press).
27. Dyke, A. S. & Prest, V. K. Late Wisconsinan and Holocene history of the Laurentide ice sheet. *Géogr. Phys. Quat.* **41,** 237–264 (1987).
28. Vinje, T., Nordlund, N. & Kvambekk, A. Monitoring ice thickness in Fram Strait. *J. Geophys. Res.* **103,** 10437–10449 (1998).
29. Fairbanks, R. G. A 17,000-year glacio-eustatic sea level record: influence of glacial melting rates on the Younger Dryas event and deep-ocean circulation. *Nature* **342,** 637–641 (1989).
30. Tarasov, L. & Peltier, W. R. Greenland glacial history, borehole constraints and Eemian extent. *J. Geophys. Res.* **108,** 2124–2143 (2003).

Supplementary Information is linked to the online version of the paper at www.nature.com/nature.

Acknowledgements This paper is a contribution to the Polar Climate Stability Research Network, which is funded by the Canadian Foundation for Climate and Atmospheric Sciences and a consortium of Canadian universities. We thank W. Broecker, A. Dyke, T. Fisher, C. Hillaire-Marcel and J. Teller for discussions.

Author Information Reprints and permissions information is available at npg.nature.com/reprintsandpermissions. The authors declare no competing financial interests. Correspondence and requests for materials should be addressed to L.T. (lev@atmosp.physics.utoronto.ca).